Stability and electronic structure of the (1×1) $SrTiO_3(110)$ polar surfaces by first-principles calculations

François Bottin, Fabio Finocchi, and Claudine Noguera
Groupe de Physique des Solides, Universités Paris 6 - Paris 7 et UMR CNRS 7588, 2 place Jussieu, 75251 Paris cedex 05, France
(Received 19 November 2002; revised manuscript received 24 March 2003; published 21 July 2003)

The electronic and atomic structures of several (1×1) terminations of the (110) polar orientation of the $SrTiO_3$ surface are systematically studied by first-principles calculations. The electronic structure of the two stoichiometric SrTiO and O_2 terminations are characterized by marked differences with respect to the bulk, as a consequence of the polarity compensation. In the former, the Fermi level is located at the bottom of the conduction band, while in the latter the formation of a peroxo bond between the two surface oxygens results in a small-gap insulating surface with states in the gap of the bulk projected band structure. We also consider three nonstoichiometric terminations with TiO, Sr, and O compositions, respectively, in the outermost atomic layer, which automatically allows the surface to be free from any macroscopic polarization. They are all insulating. The cleavage and surface energies of the five terminations are computed and compared, taking into account the influence of the chemical environment as a function of the relative richness in O and Sr. From our calculations, it appears that some (110) faces can even compete with the TiO_2 and SrO terminations of the (100) cleavage surface: in particular, the (110)-TiO termination is stable in Sr-poor conditions, the (110)-Sr one in simultaneously O- and Sr-rich environments. The available experimental data are compared to the outcomes of our calculations and discussed.

DOI: 10.1103/PhysRevB.68.035418 PACS number(s): 68.47.Gh, 31.15.Ar, 73.20.At, 68.35.Bs

I. INTRODUCTION

Strontium titanate is a material that has many potential applications. Its high dielectric constant makes it a candidate to replace silicon dioxide in some nanoelectronic devices. $SrTiO_3$ has been used in photoelectrolysis and as a substrate for the growth of high-T_c superconductors as well as of other thin oxide films.[1] Like other perovskite compounds, $SrTiO_3$ shows a rich physical behavior. It undergoes an antiferrodistortive (AFD) transition at $T<105$ K: the cubic structure turns into a tetragonal phase, where the neighboring TiO_6 octahedra are tilted with opposite angles around a [100] direction, doubling the unit cell. Moreover, $SrTiO_3$ is at the boundary of a ferroelectric transition,[2–4] but remains paraelectric for all temperatures.[5]

While the (100) surfaces of $SrTiO_3$ have been extensively studied, both theoretically[6–8] and experimentally,[9–11] the (110) terminations are much less known. Such a scarcity is likely due to the polar character of the (110) orientation. The sequence of atomic layers of O_2 and SrTiO stoichiometry implies a monotonic raise of the microscopic electric field, which has to be compensated either through a modification of the surface composition—which leads to nonstoichiometric terminations—or by an anomalous filling of the surface electronic states—which must imply crucial variations of the electronic structure of the surfaces that should be, in principle, detectable by experiments.

Nevertheless, {110} terminations of strontium titanate have been observed quite often, but the effort towards the precise characterization of their atomic-scale morphology and the detailed study of the corresponding electronic structures started only in the last decade. For instance, it is worth noting the investigations by atomic force microscopy,[12] scanning tunneling microscopy (STM), Auger spectroscopy and low-energy electron-diffraction (LEED) measurements,[13] as well as ultraviolet photoemission and x-ray photoemission spectroscopies (UPS and XPS, respectively), coupled to LEED.[14] In the latter works, the authors made a considerable effort to characterize the modifications of the electronic structure, which are connected to different preparation conditions of the surface through STM and scanning tunneling spectroscopy[15] angle-resolved photoemission,[16] and conduction measurements.[17] Not all of these studies provide a unifying picture of the surface, which indeed shows a great sensitivity to the thermodynamic conditions, mainly temperature and oxygen partial pressure.

Motivated by this experimental works, some theoretical studies of $SrTiO_3(110)$ recently appeared. The optimized surface geometry was obtained through interatomic forces that were derived either by an empirical shell model,[18] or by more accurate treatments that are based on the Hartree-Fock approximation, still describing the Hamiltonian matrix on semiempirical grounds.[19,20] The approximate nature of these approaches allowed some trends to be deduced, but it did not permit, in most cases, to draw quantitative conclusions that could be compared to experiments. On the other hand, first-principles approaches that are based on the density-functional theory (DFT) have been widely applied to the study of oxide surfaces in recent years. More specifically to perovskite surfaces, such an approach has been showed to be reliable and complementary to experiments.[7] It is the aim of the present paper to provide an application of state-of-the-art first-principles methods to the (110) polar termination of $SrTiO_3$, which is the first one to the best of our knowledge.

In particular, we focus on two issues: (i) Which is the mechanism at work to cancel the macroscopic polarization? (ii) Is the thermodynamic stability of the (110) termination comparable to that of the (100) cleavage face? Regarding (i),

while in the wide-gap rocksalt compounds MgO and NaCl the nonstoichiometric reconstructions, such as the octopolar one, are clearly favored over polarity compensation by an anomalous filling of surface states, it has been recently suggested for the less ionic ZnO(0001) and ZnO($000\bar{1}$) surfaces[21,22] that the latter mechanism may work. The coexistence of the rather ionic Sr-O bonds with the more covalent Ti-O ones, as well as the fairly large dielectric constant of $SrTiO_3$ might situate strontium titanate at the borderline between the two previous cases. Regarding (ii), the quite numerous observations of {110} (1×1) terminations suggest that these surfaces may be obtained in appropriate thermodynamic conditions. However, the ternary nature of strontium titanate, as well as the lack of precise experimental indications on the surface composition, make the first-principles modeling a rather delicate task. Therefore, in this work, we restrict ourselves to several terminations, stoichiometric or not, of (1×1) reconstructions, completing a previous preliminary report:[23] the two stoichiometric O_2 and SrTiO faces, and the three nonstoichiometric O, TiO, and Sr terminations. Their atomic and electronic structures are computed and discussed in Sec. III. Moreover, their relative stabilities are compared as functions of the chemical environment (see Secs. IV and V).

II. COMPUTATIONAL METHOD

The calculations are carried out within the DFT.[24] The exchange and correlation energy is treated via the local-density approximation (LDA) using the Perdew-Wang parametrization.[25] The Kohn-Sham orbitals are expanded on a plane-wave (PW) basis set and an energy cutoff of 30 hartree (Ha) is employed. For all calculations, we use the ABINIT computer code.[26]

In conjunction with the use of a PW basis set, we adopt soft norm-conserving pseudopotentials that are generated by following the Troullier-Martins scheme[27] in the Kleinman-Bylander form[28] in order to avoid taking into account the inner atomic electrons in the self-consistent cycle explicitly. Along the pseudopotential generation process, atom reference states $3d^1 4s^{0.5} 4p^{0.25}$ for Ti, $4s^2 4p^6 5p^1$ for Sr, and $2s^2 2p^4$ for O are used. The pseudization radii are $R_c(s) = 2.45$ bohr, $R_c(p) = 2.55$ bohr, and $R_c(d) = 2.25$ bohr for Ti; $R_c(s)2.0$ bohr, $R_c(p) = 2.5$ bohr, and $R_c(d) = 2.2$ bohr for Sr; and $R_c(s) = R_c(d) = 1.4$ bohr and $R_c(p) = 1.75$ bohr for O, with *s*, *p*, and *d* being the different channels. The Sr $4s$ and $4p$ semicore electrons are treated as valence electrons in the self-consistent procedure, (which we refer to in the following as the small-core approximation), whereas the Ti $3s$ and $3p$ semicore states are frozen (large-core approximation). Since the latter states have an appreciable superposition with the $4s$ and $3d$ radial orbitals of Ti, in the exchange and correlation functional we take into account the nonlinear core correction[29] between the radial density corresponding to the frozen $3s$ and $3p$ Ti orbitals and the valence electron density.

The previously described computational scheme is tested on the cubic phase of bulk $SrTiO_3$. The lattice parameter a_0, the bulk modulus B_0, and the cohesive energy E_{coh} are very close to the experimental data (see Table I). The large-core approximation for Ti is also checked against the small-core one, and the former is adopted in all slab calculations. The gap between the valence and the conduction band computed through the difference of the Kohn-Sham eigen-energies (2.1 eV) is smaller than the experimental value (3.2 eV),[30] which is a common case for the DFT.[31]

TABLE I. Experimental and computed lattice parameter a_0, bulk modulus B_0, and cohesive energy E_{coh} for the cubic $SrTiO_3$ phase. The experimental values of a_0 and E_{coh} are quoted in Ref. 32 and B_0 is taken from Ref. 33. Two distinct calculations adopting the small-core and large-core approximations for the Ti pseudopotential (see text) are also shown.

	Calc. (large core)	Calc. (small core)	Experiment
a_0 (Å)	3.951(+1.2%)	3.875(−0.8%)	3.903
B_0 (Gpa)	187(+2%)	192(+5%)	183
E_{coh} (eV)	34.06(+7%)	37.00(+17%)	31.7

The calculated formation energies of bulk Ti and Sr from the isolated atomic species are $E^f_{\mathrm{Ti}} = 4.58$ eV and $E^f_{\mathrm{Sr}} = 1.73$ eV, which differ by −6% and +2% from the experimental values, respectively. On the other hand, the O_2 formation energy ($E^f_{\mathrm{O}_2} = 7.58$ eV) is about 45% greater than the experimental value, like in previous LDA calculations.[34]

The surfaces are described in the framework of the slab model. The calculations are carried out by sampling the irreducible Brillouin zone by a (4,4,2) Monkhorst-Pack mesh.[35] By using a (5,5,2) mesh, the computed total energies decrease by less than 10 meV for the insulating terminations and 20 meV for the metallic ones. In these cases, when an effective Fermi-surface smearing is employed to get a better convergence,[36] a careful procedure is used to extrapolate convergent energies in the limit $T\rightarrow0$. The stable surface configurations is obtained by minimizing the Hellmann-Feymann forces in the Born-Oppenheimer approximation, generally starting from the geometry of the ideal unrelaxed surfaces.

In order to avoid spurious interaction between periodic slabs via dipole-dipole interactions,[37,38] the compositions of the adopted slabs are symmetric upon inversion along the surface normal. Well converged slab total energies can be routinely obtained for typical vacuum widths ranging between 10 and 12 Å. On the other hand, the determination of the minimal number of atomic layers that is allowed needs some care. For instance, a nine-layer slab is sufficient for the two nonstoichiometric (110)-Sr and (110)-TiO terminations, whereas 11 layers are at least needed for the two (110)-O_2 and (110)-SrTiO stoichiometric terminations. In the case of the O-terminated surfaces, a very careful choice of the bulk reference energy is also needed, as detailed in the following. To this purpose, we made calculations up to 15-layer thick slabs. As a general rule, the slab is considered to be thick enough when the difference between the total energies of two slabs differs by a $SrTiO_3$ unit and the bulk total energy is smaller than 1 mHa.[54] This condition cancels out the problem of nonconvergent surface energies,[39,40] and makes it pos-

sible to obtain a fair bulk reference energy for each termination.

Even if our calculations are carried out at 0 K, we impose symmetry constraints to our slabs to simulate the cubic phase that is stable at room temperature. A special case is represented by the nonstoichiometric (110)-O termination, since the mirror symmetry along the $[\bar{1}10]$ direction is lost. As it will be detailed in the section devoted to such a termination, the bulk energy should be computed with reference to an AFD phase that is simulated in a tetragonal supercell analogous to that used for the slab. Other authors gave details about the change of the AFD distortion with respect to the bulk structure.[41] Our computed total-energy differences between the cubic and the AFD phases is about 2 mHa. Neglecting such a small quantity may appreciably bias the numerical extrapolation of the surface energy when a linear scheme is used. To summarize, the uncertainty on the surface energies E_{cl} within our slab approach does not exceed 10^{-2} J/m^2, which is usually much smaller than the computed surface energy differences for the various terminations.

We also focus on the total electron distribution in the various surface configurations. An estimate of the electron sharing between the O anions and the Sr and Ti cations is obtained by means of Bader's topological analysis of the electron density, which corresponds to a partition of the total charge in atomic basins. Such a procedure is independent of the basis set used,[42] and has been recently used[43] and improved within the ABINIT package. The precision of the atomic charge integration is about 5×10^{-3} electrons.

III. ELECTRONIC AND ATOMIC STRUCTURE

In the (110) orientation of $SrTiO_3$, a stacking sequence of atomic layers $\cdots O_2$-SrTiO-O_2-SrTiO$\cdots$ is provided. If we consider that the ionic charge of O, Ti, and Sr are $Q_O=-2$, $Q_{Ti}=+4$, and $Q_{Sr}=+2$, respectively, then the O_2 plane bears a formal charge $Q_{O_2}=-4$ and the SrTiO plane $Q_{SrTiO}=+4$ per two-dimensional unit cell. According to the criterion for polarity compensation,[44,43] the formal surface charges of the various $SrTiO_3$(110) faces have to be equal to half the bulk value, i.e., $Q_{surf}=\pm2$. Therefore, we consider two main classes of (1×1) terminations: on one side, the so-called stoichiometric terminations, since their compositions reflect the bulk stacking, namely, the (110)-SrTiO and $-O_2$ ones, for which an anomalous filling of surface states is expected. On the other side, we study the (110)-TiO, -Sr, and -O terminations, for which the stoichiometry changes can, in principle, provide the polarity compensation. For each termination, we describe in the following the detailed atomic and electronic structures.

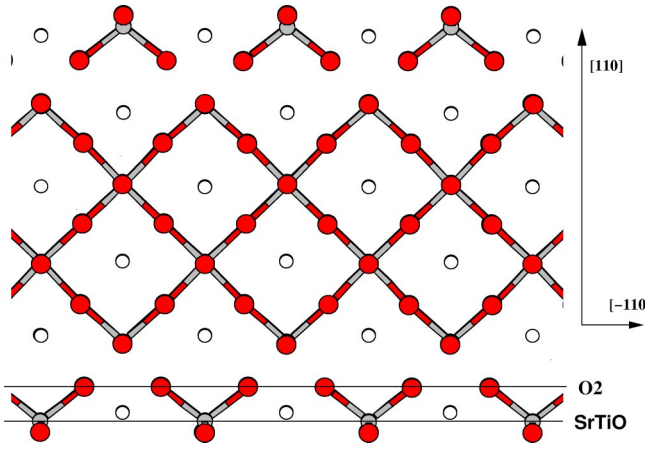

FIG. 1. (Color online) Side view of the SrTiO slab cut along a [001] plane. Sr, Ti, and O atoms are white, gray, and red, respectively.

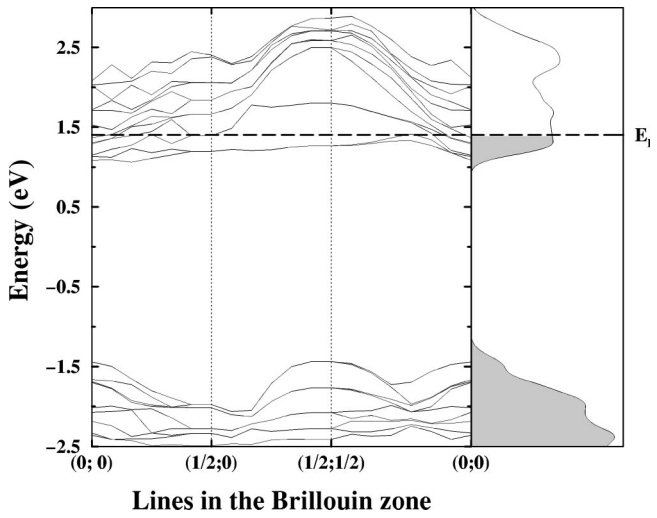

FIG. 2. Computed band structure for the SrTiO termination of $SrTiO_3$(110). Only the valence-band top and the conduction-band bottom are drawn.

A. Stoichiometric terminations

1. The SrTiO termination

In the stoichiometric (110)-SrTiO termination (see Fig. 1), six Sr-O bonds and two Ti-O bonds are cut. Since the surface plane bears a formal charge $Q_{SrTiO}=+4$, there must be an anomalous filling of surface states, in order to cancel out the macroscopic component of the slab dipole.[44] Figure 2 reports the computed band structure. One can note that the

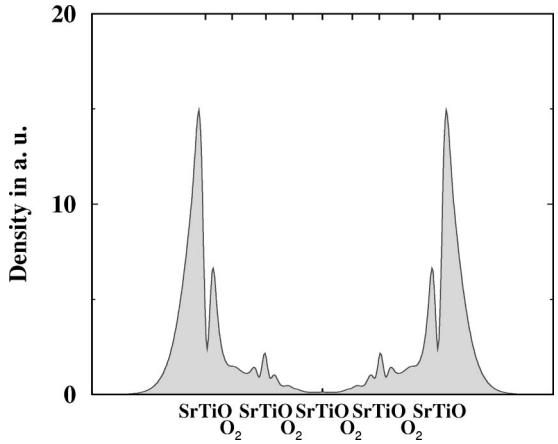

FIG. 3. Localization of the compensatory state at the *M* (0.5;0.5;0.0) point of the Brillouin zone.

TABLE II. q_O, q_{Ti}, and q_{Sr} are Bader's topological charges of oxygen, titanium, and strontium, respectively for the SrTiO termination. I, II, III, and IV give the indices of the layer. Charge is given in electron number. For comparisons, bulk values are given at the bottom.

Layer	Atomic charges	Layer charge
SrTiO	$q_O^I=-1.36$; $q_{Ti}^I=1.74$; $q_{Sr}^I=1.40$	$q_{SrTiO}^I=1.78$
O_2	$q_O^{II}=-1.38$	$q_{O_2}^{II}=-2.76$
SrTiO	$q_O^{III}=-1.30$; $q_{Ti}^{III}=2.03$; $q_{Sr}^{III}=1.55$	$q_{SrTiO}^{III}=2.28$
O_2	$q_O^{IV}=-1.30$	$q_{O_2}^{IV}=-2.60$
Bulk	$q_O^{Bulk}=-1.26$; $q_{Ti}^{Bulk}=2.18$; $q_{Sr}^{Bulk}=1.58$	$q^{Bulk}=2.50$

TABLE III. Relaxation and rumpling on the (110)-SrTiO termination. The mean positions of the SrTiO layers are computed by averaging the normal coordinates of the corresponding atoms. The interplanar distances are given in angstroms and their relative variations in brackets.

Layer	Relaxations and rumplings
SrTiO	Ti(−0.03) O(+0.38) Sr(−0.35)
↕	1.25(−11%)
O_2	No rumpling
↕	1.66(+19%)
SrTiO	Ti(+0.06) O(+0.13) Sr(−0.19)
↕	1.28(−8%)
O_2	No rumpling
↕	1.49(+6%)
SrTiO	Ti(+0.01) O(+0.04) Sr(−0.05)
↕	1.38(−1%)
O_2	No rumpling

Fermi energy is located above the bottom of the conduction band. Some conductionlike states are thus filled, which bring the two additional electrons that are needed according to the electron counting rule for polarity compensation.

These states are localized in the outermost layers and are genuine surface states. The density of the filled conduction-band state at the *M* point of the Brillouin zone, that is displayed in Fig. 3, is roughly delocalized over three surface layers, which shows that the self-consistent charge redistribution is more complex than the model that is based upon the values of the formal ionic charges. A more thorough insight can be obtained by means of Bader's topological charge analysis, which is reported in Table II. The layer charge $q_{SrTiO}^{I,III}$ and $q_{O_2}^{II}$ of the first and third SrTiO and the second O_2 outermost planes, respectively, are indeed strongly modified by the filling of the additional surface state and thus show marked changes from the computed charge for the inner bulklike layers ($q^{Bulk}=\pm 2.50$), which is roughly achieved only in the fourth layer. The polarity compensation criterion is fulfilled, since the sum of the charge of the four first layers is equal to -1.30, which is almost the half of the bulk layer charge q^{Bulk}.

Finally, we can see in Table II that the difference between the surface layer charge q_{SrTiO}^I and the bulk layer charge q^{Bulk} is mainly localized on titanium, which is confirmed by the direct visualization of the filled state at the conduction-band bottom (in the right part of Fig. 4). However, an effective decrease of the electronic kinetic energy may be obtained through the delocalization of this state over neighboring sites. Such a screening phenomenon, reminiscent to that found in Na-covered $TiO_2(110)$ surfaces,[45] thus affects the Sr and O charges, too. The charge of the outermost Ti is thus reduced, which can be probed by XPS experiments through a surface Ti signal that should differ from the bulk Ti^{4+} formal oxidation state to a large extent.

As far as the atomic structure is concerned, we can see in Table III that large relaxations occur in the four outermost layers. For instance, the large rumpling between oxygen and strontium that is equal to 0.73 Å in the surface layer is still non-negligible in the third layer (0.32 Å). The interplanar distance between the outermost SrTiO layer and the O_2 layer beneath it contracts by 11%, while that between the latter and the third SrTiO planes grows by +19%, showing a typical damped oscillation that makes each pair of surface unlike layers closer, as accounted for by the general theory.[46,47] However, the surface Ti-O bond lengths $d_{Ti\text{-}O}$ are only weakly modified: for Ti in the topmost layer, $d_{Ti\text{-}O}$ is reduced by −3%, while it is expanded by 5% in the third layer. Such a behavior is due to the combined relaxation and rumpling that mainly rotate the Ti-O bond. At odds, the more ionic and

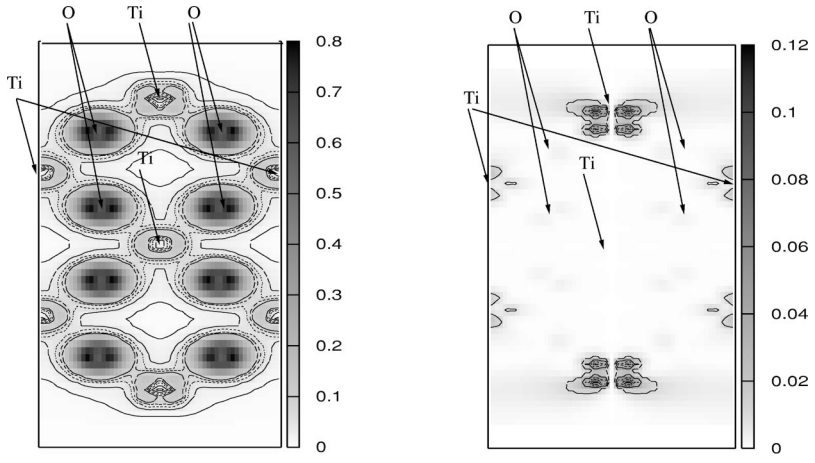

FIG. 4. Cutting of the total valence density (left) and compensatory state density (right) perpendicular to the [100] direction in a TiO_2 plane.

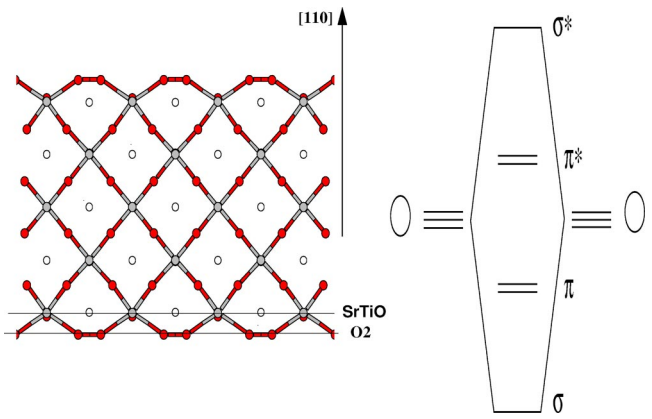

FIG. 5. (Color online) Left part: side view of the O_2-$SrTiO_3$(110) slab, cut perpendicular to the [001] crystallographic direction. Right part: schematic molecular diagram of an oxygen dimer. In the case of an isolated O_2^{--} group, the two π^* orbitals are completely filled.

weaker Sr-O bonds are much more affected: $d_{\mathrm{Sr^I\text{-}O^{III}}}$ is reduced by 13%, while $d_{\mathrm{O^I\text{-}Sr^{III}}}$ is expanded by 24%.

2. The O_2 termination

The complementary stoichiometric (110)-O_2 termination is also expected to undergo large modifications of the electronic structure because of the polarity compensation, which requires two electrons to be removed from the surface. As displayed in the left part of Fig. 5, the two surface oxygens move close to each other forming a bond 1.48 Å long. Such a bond length is usually a signature of a peroxo group,[48] which is formally denoted as O_2^{2-} in the ionic limit. It would imply that the surface charge per unit cell is $Q_{surf}=-2$, instead of -4 as in the bulk. Therefore, the formation of a peroxo group formally permits to fulfill the polarity compensation criterion.

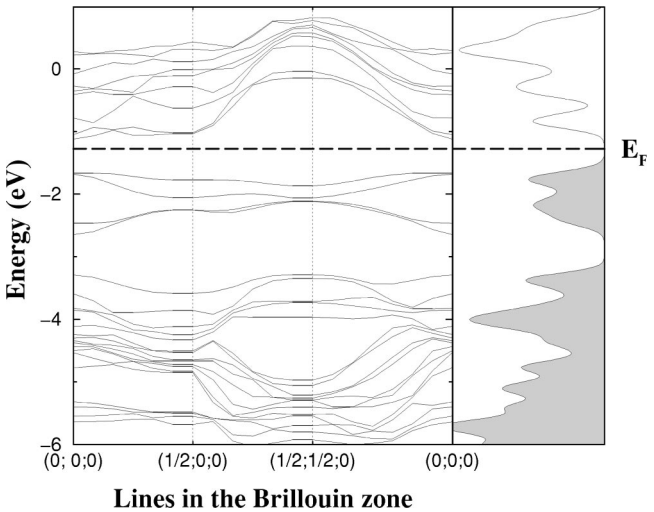

FIG. 6. Computed band structure for the O_2-terminated slab. Only the valence-band top and the conduction-band bottom are drawn. The π^* states discussed in the text give rise to four bands (two for each termination), which are not completely degenerated due to finite-slab effects.

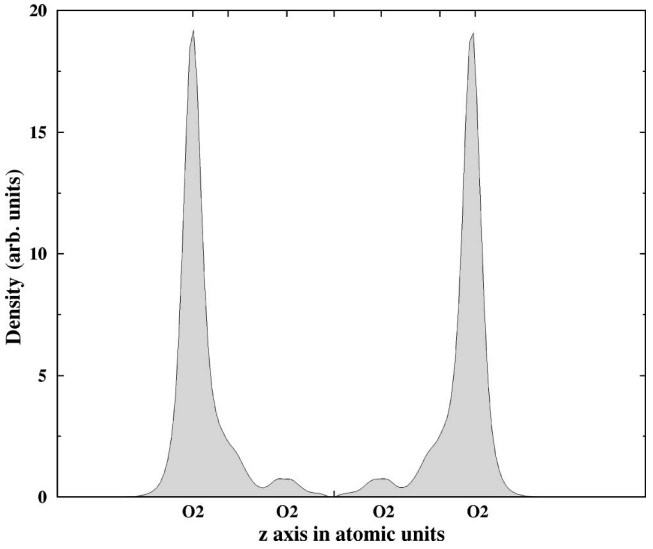

FIG. 7. Localization of the highest occupied state π^* for the O_2 termination of $SrTiO_3$(110).

Less formally, one can see that the formation of a peroxo bond is made possible by emptying the antibonding σ^* molecular orbital (see the right panel of Fig. 5). This also provides an effective mechanism to open a small gap at the surface (see Fig. 6). The Fermi level rests above the two antibonding states π^* and does not cross the band structure. The bulk gap value of $SrTiO_3$ (around 2 eV) is found between the valence band and the conduction band (i.e., excluding the O_2 π^* states). The two in-gap π^* states are split, since the two $[\bar{1}10]$ and [001] crystallographic directions are not equivalent, and are localized at the surface layer as displayed in Fig. 7.

Table IV yields the results of Bader's topological analysis for this termination. The topological charges of the surface O (O^I) are sensitively reduced, consistently with the formation of the peroxo bond. We obtain a surface charge almost equal to half the bulk one. In this case, the charge modification is essentially restricted to the outermost O atoms, as a consequence of the covalent and localized nature of the peroxo bond.

As far as the atomic structure is concerned, important modifications are present on the surface. The oxygen atoms tilt at the surface and reduce their angle with respect to the [110] direction by strongly increasing the bond length with titanium on the second layer ($d_{\mathrm{O^I\text{-}Ti^{II}}}$) by 19%. As a consequence,there is a large inward relaxation (-20%—see also Table V) of the peroxo bond with respect to the second layer.

TABLE IV. Same as Table II, for O_2 termination.

Layer	Atomic charges	Layer charge
O_2	$q_{\mathrm{O}}^{I}=-0.66$	$q_{\mathrm{O_2}}^{I}=-1.32$
SrTiO	$q_{\mathrm{O}}^{II}=-1.20$; $q_{\mathrm{Ti}}^{II}=2.13$; $q_{\mathrm{Sr}}^{II}=1.55$	$q_{\mathrm{SrTiO}}^{II}=2.48$
O_2	$q_{\mathrm{O}}^{III}=-1.21$	$q_{\mathrm{O_2}}^{III}=-2.42$
SrTiO	$q_{\mathrm{O}}^{IV}=-1.24$; $q_{\mathrm{Ti}}^{IV}=2.19$; $q_{\mathrm{Sr}}^{IV}=1.58$	$q_{\mathrm{SrTiO}}^{IV}=2.53$
Bulk	$q_{\mathrm{O}}^{Bulk}=-1.26$; $q_{\mathrm{Ti}}^{Bulk}=2.18$; $q_{\mathrm{Sr}}^{Bulk}=1.58$	$q^{Bulk}=-2.50$

TABLE V. Same as Table III, for O_2 termination.

Layer	Relaxations and rumplings
O_2	No rumpling
↕	1.12(−20%)
SrTiO	Ti(−0.05) O(+0.12) Sr(−0.07)
↕	1.52(+9%)
O_2	No rumpling
↕	1.32(−6%)
SrTiO	Ti(−0.02) O(+0.03) Sr(−0.01)
↕	1.45(−4%)
O_2	No rumpling
↕	1.40(0%)
SrTiO	No rumpling

On the other hand, $d_{O^{I}\text{-}Sr^{II}}$ is remarkably reduced (−13%).

We point out that a few surface configurations were obtained for the (110)-O_2 termination through the minimization procedure. The one reported in Fig. 5 has the lowest total energy. Another configuration with the peroxo group on top of the titanium is found, which is slightly higher in energy (5×10^{-3} J/m^2), but still within the intrinsic precision of our calculations. These two configurations have very similar band structures and atomic charges, and can be considered as almost degenerated. It is worth noting that when starting the geometry optimization from the ideal, unrelaxed (110)-O_2 termination, a third local minimum without peroxo groups at the surface is found. With respect to the peroxo configurations, it has an open-shell structure and a higher surface energy of about 0.7 J/m^2.

B. Nonstoichiometric terminations

The (110)-TiO, -O, and -Sr terminations may be ideally obtained from the stoichiometric surface by adsorption or desorption of Sr and O atoms. They bear a formal charge $Q_{TiO}=+2$, $Q_O=-2$, and $Q_{Sr}=+2$ in the ionic limit, respectively, which corresponds to half the bulk layer charge $Q_{bulk}=\pm4$. Therefore, they are all compensated and no anomalous filling of surface states is, in principle, necessary. In order to demonstrate this assumption, the computed density of states of these three nonstoichiometric terminations are drawn in Fig.8. They are all insulating, with electronic structures qualitatively similar to the bulk.

1. The Sr and TiO terminations

The (110)-Sr termination is obtained from the O_2 one by adsorbing a Sr atom per unit cell whereas the (110)-TiO one is obtained from the (110)-SrTiO termination by removing a row of surface Sr along the [100] direction. These two terminations are displayed in Fig. 9.

These two (110) terminations are representative of more open surfaces. The coordination numbers of the surface atoms are reduced with respect to the stoichiometric (110)(1 ×1) terminations as well as to the nonpolar (100) surfaces. Let us imagine to cleave a $SrTiO_3$ slab along different orientations: two complementary terminations are obtained, for which a certain number of bonds are missing. Such cut bonds are four Sr-O and one Ti-O for the nonpolar (100) orientation; Two Ti-O and six Sr-O bonds for the (110)-SrTiO and (110)-O_2 terminations, as well as for the (110)-O termination, which is self-complementary; Two Ti-O and eight Sr-O bonds for the (110)-TiO and (110)-Sr terminations. Moreover, the (110)-Sr and (110)-TiO terminations have an uncoordinated atom even in the third layer starting from the surface (a Sr-O bond is cut), at variance with the (100)-TiO_2, 100-SrO, and the (110)-SrTiO, (110)-O_2, (110)-O terminations. Therefore, it is not surprising that the remaining atoms on the (110)-Sr and (110)-TiO undergo large relaxations (see Table VI), such as the inward relaxation of the surface Sr on the Sr termination (−43%) and the strong rumpling of the Ti and O atoms on the TiO termination (0.48 Å). Despite this undercoordination, relaxations are more quickly damped than for the stoichiometric terminations. For instance, the interplanar relaxation between the third and the fourth layer is reduced by a factor of 2 with respect to the stoichiometric (110)-SrTiO and (110)-O_2 terminations.

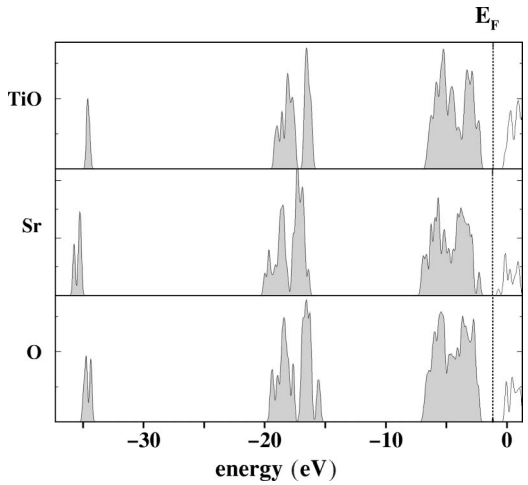

FIG. 8. Density of states of the TiO, Sr, and O terminations. The occupied states are filled in gray, and E_F is the Fermi level.

Since the (110)-Sr and the (110)-TiO terminations are intrinsically compensated by stoichiometry, we may guess that the atomic surface charges differ little from the bulk, and that such an effect is mainly due to the reduction of the surface-atom coordination numbers. In fact, Bader's topological analysis (see Table VII) confirms the polarity compensation of the two terminations: the charge modification affects essentially the three outermost layers and their sum on these layers is equal to +1.21, which is almost half of the bulk value. Even if these changes are less intense than on the stoichiometric terminations, they extend rather deeply into the slabs, which confirms the correlation with the presence of undercoordinated atoms and the interplay between the atomic relaxations and the electron redistribution.

2. The O termination

Such a termination may be ideally obtained in two different ways: by removing an oxygen atom from an O_2 termina-

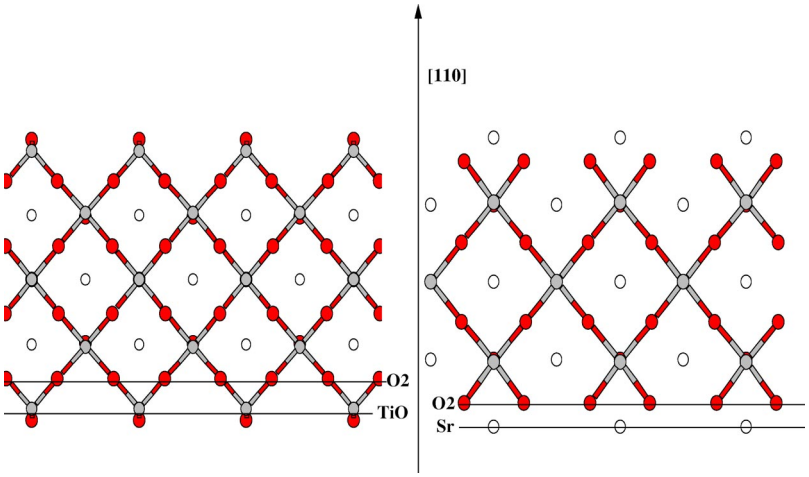

FIG. 9. (Color online) Left (right) panel: side view of the TiO (Sr) slab, cut along a [001] plane.

tion or by adding an oxygen atom on a SrTiO termination. The presence of a single O atom on the surface breaks the mirror symmetry along the $[\bar{1}10]$ direction, at odds with all (1×1) terminations that were previously considered. Consequently, among all the (110) terminations, the convergence of the atomic structure and the surface energy of this one is the most difficult. We can see in Fig. 10 that the broken surface symmetry permits a distortion and its propagation into the slab. It consists of an alternating rotation of the octahedra along a [100] direction, which is known as an AFD instability. We point out that such an abnormal deep propagation of the AFD instability from the surface into the bulk is related to the fact that the low-symmetry phase is stable at $T=0$ K, the temperature for which the calculations are performed. This propagation may be hindered by considering a 15-layer slab with five inner layers frozen. Even in this case, the surface atomic structure is practically indistinguishable from that obtained on top of an AFD bulk.

The surface O relaxes inwards (-33%) and laterally toward the two strontium atoms underneath (see Table VIII). In the inner part of the slab, no large interplanar relaxation occurs. However, a quite strong rumpling affects the inner O_2 layers, which corresponds to the AFD distortion and is not damped as a function of the slab thickness. Moreover, there are large lateral atomic displacements within the SrTiO layers that are denoted with δ_{TiO_2} (see Table VIII) and decrease quite rapidly going into the bulk. As a consequence of this distortion, the O-Ti-O alignment is broken along the [001] direction. The topological charges of the surface oxygen atoms are very similar to the bulk ones from which they differ by 10% at most.

IV. THERMODYNAMIC STABILITY

Because of the different chemical nature of the various (1×1) (110) terminations of $SrTiO_3$, their stability must be discussed as a function of the actual surface composition.[7,19,49,50] To this purpose, we make use of two distinct physical quantities: the first one corresponds to the energy that is necessary to split the crystal into two parts and create two complementary terminations, which we refer to as the cleavage energy E_{cl}. The second one is the surface grand potential Ω_s^i, which is a measure of the excess energy of a semi-infinite crystal exposing a termination with a given composition i in contact with matter reservoirs.

A. Cleavage energy

When a stoichiometric $SrTiO_3$ slab is ideally cut and the two parts are put apart, two complementary surface terminations are created. In our case, they are the (110)-SrTiO and the (110)-O_2 terminations on one hand, and the (110)-TiO and the (110)-Sr ones on the other. The (110)-O termination can be considered as self-complementary. The respective

TABLE VI. Same as Table III, but for the (110)-TiO and (110)-Sr terminations.

Layer	Relaxations (TiO)	Relaxations (Sr)
TiO/Sr	Ti(−0.24) O(+0.24)	No rumpling
↕	1.51(+8%)	0.79(−43%)
O_2	No rumpling	No rumpling
↕	1.43(+2%)	1.53(+10%)
SrTiO	Ti(+.08) O(−.07) Sr(−.01)	Ti(+.06) O(−.02) Sr(−.04)
↕	1.32(−5%)	1.35(−4%)
O_2	No rumpling	No rumpling
↕	1.40(0%)	1.41(+1%)
SrTiO	No rumpling	No rumpling

TABLE VII. Same as Table II for the (110)-TiO termination. For the (110)-Sr termination, the topological charges of the surface atoms are very similar to the bulk ones, from which they differ by 7% at most.

Layer	Atomic charges	Layer charge
TiO	$q^{I}_{O}=-1.20$; $q^{I}_{Ti}=2.04$	$q^{I}_{TiO}=0.84$
O_2	$q^{II}_{O}=-1.11$	$q^{II}_{O_2}=-2.22$
SrTiO	$q^{III}_{O}=-1.20$; $q^{III}_{Ti}=2.21$; $q^{III}_{Sr}=1.58$	$q^{III}_{SrTiO}=2.59$
O_2	$q^{IV}_{O}=-1.25$	$q^{IV}_{O_2}=-2.50$
Bulk	$q^{Bulk}_{O}=-1.26$; $q^{Bulk}_{Ti}=2.18$; $q^{Bulk}_{Sr}=1.58$	$q^{Bulk}=-2.50$

cleavage energies $E_{cl}^{(O_2+SrTiO)}$ and $E_{cl}^{(TiO+Sr)}$ can be obtained from the total energies computed for the symmetric slabs through the following equations:

$$E_{cl}^{(TiO+Sr)}=\frac{1}{2S}(E_{slab}^{TiO}+E_{slab}^{Sr}-nE_{bulk}), \quad (1)$$

$$E_{cl}^{(O_2+SrTiO)}=\frac{1}{2S}(E_{slab}^{O2}+E_{slab}^{SrTiO}-nE_{bulk}), \quad (2)$$

where E^{i}_{slab} the total energy of the symmetric slab with the *i* termination, *n* the total number of bulk formula units in the two slabs, *S* the surface area, and E_{bulk} the bulk energy per formula unit in the cubic structure.

Since the (110)-O termination is self-complementary and shows an AFD distortion, its cleavage energy $E_{cl}^{(O+O)}$ is calculated by using a unit factor instead of one-half and a different reference energy E^{AFD}_{bulk} that reads

$$E_{cl}^{O+O}=\frac{1}{S}(E_{slab}^{O}-nE_{bulk}^{AFD}). \quad (3)$$

As previously pointed out in Sec. II, a different choice for the reference energy would result in an ill-defined cleavage energy. This is exemplified in a recent calculation, in which an apparently diverging cleavage energy was obtained for the (110)-O termination[18] by using the cubic, undistorted reference energy, instead of E^{AFD}_{bulk}. Our numerical results are summarized in Table IX. The O termination has the lowest cleavage energy (2.54 J/m^2), whereas O_2 and SrTiO have the highest one (6.52 J/m^2). We also note that the three nonstoichiometric terminations have lower cleavage energies than the two stoichiometric ones. Consequently, the polarity compensation that is achieved through the modification of the surface stoichiometry seems to be more effective than that by the anomalous filling of the surface states, as far as energetics is concerned.

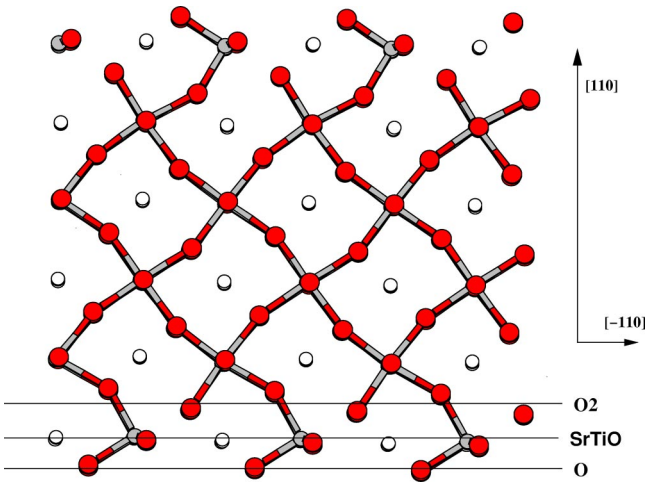

FIG. 10. (Color online) Side view of the (110)-O slab.

TABLE VIII. Relaxation and rumpling on the (110)-O termination. The mean positions of the SrTiO layers are computed by averaging the normal coordinates of the corresponding atoms. The interplanar distances are given in angstroms and their relative variations in brackets. δ_{TiO_2} corresponds to the Ti-O lateral relaxation (the projected interatomic distance along the $[\bar{1}10]$ direction).

Layer	Relaxations and rumpling	δ_{TiO_2}
O		
↕	0.94(−33%)	
SrTiO	Ti(−0.09) O(+0.06) Sr(+0.03)	0.391
↕	1.42(+2%)	
O_2	O(±0.33)	
↕	1.38(−1%)	
SrTiO	Ti(+0.05) O(+0.02) Sr(−0.08)	0.087
↕	1.38(−1%)	
O_2	O(±0.23)	
↕	1.376(−1%)	
SrTiO	Ti(−0.03) O(0.00) Sr(−0.03)	0.057
↕	1.40(0%)	
O_2	O(±0.25)	

B. The surface grand potential

In order to distinguish the contribution of each termination to the cleavage energy, we compute its surface grand potential, which implies a contact with matter reservoirs. Many authors have recently used this method with success, as well for binary[49,50] as for ternary compounds.[7,19] We introduce the chemical potential μ_{Ti}, μ_{Sr}, and μ_O of the Ti, Sr, and O atomic species, respectively. The surface grand-potential per unit area, Ω^i, of the *i* termination reads:[55]

$$\Omega^{i}=\frac{1}{2S}[E^{i}_{slab}-N_{Ti}\mu_{Ti}-N_{Sr}\mu_{Sr}-N_{O}\mu_{O}], \quad (4)$$

with N_{Ti}, N_{Sr}, and N_O the number of Ti, Sr, and O atoms in the slab and the factor of $\frac{1}{2}$ corresponds to the surface grand potential by termination. The chemical potential μ_{SrTiO_3} of a condensed and stoichiometric phase of strontium titanate is

TABLE IX. The cleavage energies E_{cl} in J/m^2.

	O+O	TiO+Sr	SrTiO+O_2
E_{cl}	2.54	3.86	6.52

TABLE X. The surface energy ϕ_i, as defined in Eq. (7), is given for each termination i in J/m^2.

i	O	TiO	Sr	SrTiO	O_2
ϕ_i	1.27	6.88	−3.01	4.78	1.73

written as a sum of three terms representing the chemical potential of each species within the crystal:

$$\mu_{SrTiO_3} = \mu_{Sr} + \mu_{Ti} + 3\mu_O. \quad (5)$$

Since the surface is in equilibrium with the bulk $SrTiO_3$, we have $\mu_{SrTiO_3} = E_{bulk}$. If we replace Eq. (5) with Eq. (4), we can eliminate the μ_{Ti} and μ_{SrTiO_3} variables in the surface grand potential and obtain

$$\Omega_s^i = \frac{1}{2S}[E_{slab}^i - N_{Ti}E_{bulk} - \mu_O(N_O - 3N_{Ti}) - \mu_{Sr}(N_{Sr} - N_{Ti})]. \quad (6)$$

Relying upon Eq. (6), one can deduce, for each termination, the range of the accessible values of Ω_s^i if the minimum and maximum values of the O and Sr chemical potentials are known (see the Appendix).

If we introduce the variation of the chemical potentials with respect to those computed for the reference phases ($\Delta\mu_O = \mu_O - E_{O_2}^{mol}/2$ and $\Delta\mu_{Sr} = \mu_{Sr} - E_{Sr}^{bulk}$, respectively) in Eq. (6), we obtain

$$\Omega_s^i = \phi_i - \frac{1}{2S}[\Delta\mu_O(N_O - 3N_{Ti}) - \Delta\mu_{Sr}(N_{Sr} - N_{Ti})]$$

$$\text{with } \phi_i = \frac{1}{2S}\left[E_{slab}^i - N_{Ti}E_{bulk} - \frac{E_{O_2}^{mol}}{2}(N_O - 3N_{Ti}) - E_{Sr}^{bulk}(N_{Sr} - N_{Ti})\right]. \quad (7)$$

ϕ_i measures the stability of the surface with respect to bulk $SrTiO_3$, gaseous molecular oxygen, and metallic Sr. In Table X, our *ab initio* results for ϕ_i are listed.

For two complementary terminations (TiO-Sr and SrTiO-O_2), the sum of their surface grand potentials is independent of the chemical potential and corresponds to their cleavage energy (see Table IX).

The derivation of the upper and lower bounds of $\Delta\mu_O$ and $\Delta\mu_{Sr}$ is detailed in the Appendix. Within the allowed region, we show in Fig. 11 (left panel) the (1×1) (110) terminations having the lowest surface grand potentials, which provides the stability diagram of $SrTiO_3$(110) (1×1) surfaces in a O and Sr external environment.

First of all, according to Fig. 11 (left panel), our calculations predict that only four out of the five possible terminations may be obtained. Indeed, the (110)-O_2 termination cannot be stabilized, even in very O-rich chemical environments. The Sr termination is the most stable one in O- and Sr-rich environments, as its complementary TiO face is in O- and Sr-poor conditions. The O termination shows a stability domain in moderate O and Sr environment. Finally, the stoichiometric and open-shell (110)-SrTiO termination happens to be stable in a small domain corresponding to O-poor and Sr-rich conditions. In order to discuss the existence of this small domain (at least within the theory) with respect to the precision of our calculations, we point out the following (see the right panel of Fig. 11).

(a) At the O-poor and simultaneously the Sr-rich zone boundary (i.e., $\Delta\mu_O = -5.46$ eV and $\Delta\mu_{Sr} = 0$ eV), the difference between Sr and SrTiO surface grand potentials is equal to 0.13 J/m^2, which is higher than the estimated precision 0.01 J/m^2 of our calculations.

(b) Since the area of the ($\Delta\mu_O$, $\Delta\mu_{Sr}$) domain is slightly underestimated by our first-principles calculations (see the Appendix), the consideration of the experimental boundaries would enlarge the stability domain of the SrTiO termination.

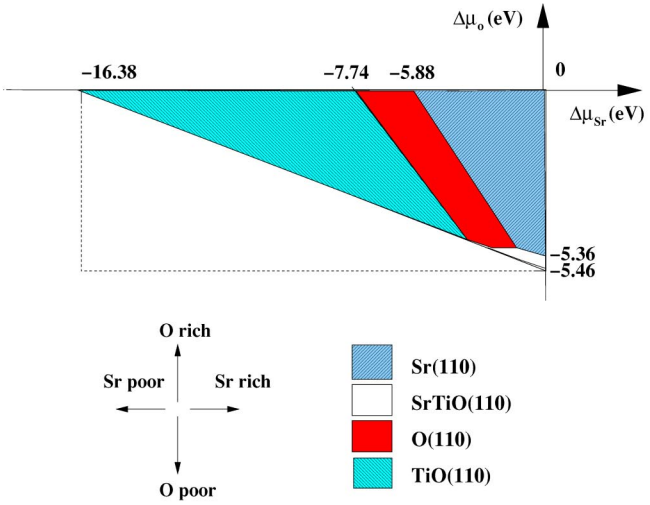

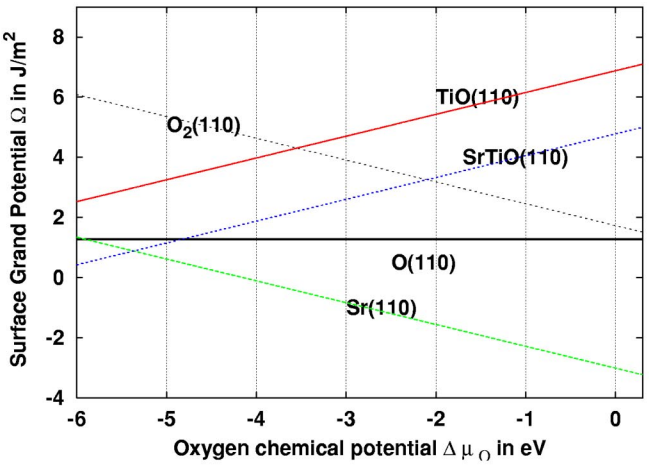

FIG. 11. (Color online) Stability diagram of the of the (1×1) $SrTiO_3$ (110) surface. The actual most stable termination is represented in the left panel as a function of the excess O and Sr chemical potentials $\Delta\mu_o$ (vertical) and $\Delta\mu_{Sr}$ (horizontal). In the right panel, the surface grand potentials are represented as functions of $\Delta\mu_O$ (for a particular value of the Sr chemical potential, $\Delta\mu_{Sr} = 0$ eV).

V. DISCUSSION

Among the questions that we raise in the Introduction, in the following we discuss three issues that are especially noteworthy.

A. A stable polar stoichiometric termination: (110)-SrTiO

We have shown in the preceding section that the (1×1) stoichiometric (110)-SrTiO termination can be stabilized in a O-poor and Sr-rich environment. Even if its stability domain comes out to be rather small, this is the second case (to our knowledge), together with the Zn and O terminations of ZnO(0001) (Ref. 21) of a stable stoichiometric polar oxide surface with an open-shell electronic structure. However, a recent STM investigation[51] questioned the proposed stoichiometric morphologies for ZnO(0001) and provides different, nonstoichiometric, structural models.

The polarity compensation through anomalous filling of surface states is expected on the basis of theoretical arguments, but it is actually not often encountered.[44] Indeed, the cleavage energies of stoichiometric polar terminations in rocksalt structures, such as the (1×1) unreconstructed (111) faces of MgO, are generally much higher than those of reconstructed, nonstoichiometric polar terminations. As a consequence, the surface grand potentials of these polar stoichiometric terminations result higher than those of the nonstoichiometric ones even when the chemical-potential-dependent terms represent a negative contribution. In this respect, the peculiar behavior of $SrTiO_3$ may be due to the presence of Ti-O covalent bonds, in conjunction with a not too large fundamental gap. Indeed, the energy increase that is due to the anomalous filling of surface states needed for polarity compensation may be effectively lessened by atomic relaxation and electronic screening effects. The latter ones show up through a nonnegligible charge transfer affecting some surface layers as supported by the analysis of the topological Bader's charge of the SrTiO termination (Table II): all Ti and O charges belonging to the three topmost layers are modified. Such a screening mechanism is less costly than a drastic charge reduction on only one or two surface atoms, which is essentially the case for MgO(111) (1×1).[52]

B. Comparison with the nonpolar $SrTiO_3(100)$ terminations

The cleavage (100) orientation of $SrTiO_3$ is nonpolar and displays two different stoichiometric terminations: the (100)-TiO_2 and the (100)-SrO. They are usually expected to be more stable than any polar face such as the (110) terminations. Indeed, within the same theoretical and computational framework, we calculated the cleavage energy of the (1×1) (100)-TiO_2 and -SrO surfaces, which is not very much lower than those of the nonstoichiometric (110) terminations. Therefore, it is worth comparing the thermodynamic stability of the simulated (1×1) (110) terminations with the two (1×1) (100)-TiO_2 and (100)-SrO faces. In Fig. 12, the domains of stability of the two (100) terminations and the five (110) terminations, previously reported, are gathered. Even if in the most common conditions, corresponding to moderate Sr and O chemical potentials, the (100) faces are

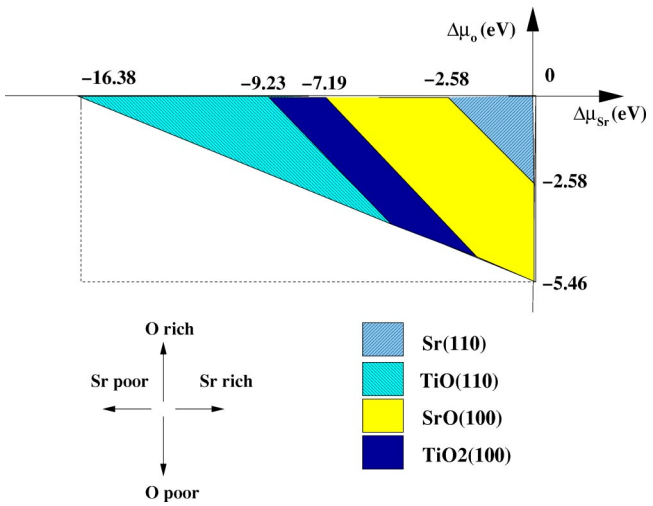

FIG. 12. (Color online) Phase diagram: comparison between the different terminations of the (1×1) $SrTiO_3$ (110) SrTiO, O_2, TiO, Sr, and O terminations and $SrTiO_3$ (100) TiO_2 and SrO terminations in a oxygen and strontium external environment.

favored, two (110) distinct (1×1) terminations are predicted to be stable—the (110)-TiO in Sr-poor environments and the (110)-Sr in O-rich and Sr-rich conditions—the first of which shows a quite wide domain of thermodynamic stability. From the theoretical point of view, the (110)-TiO and the (110)-Sr terminations can be thought of as exposing strongly relaxed {100} nanofacets (see Fig. 4). It is therefore not completely surprising that their surface energies can become comparable to those of flat {100} terraces, if the formation energy of corners and edges is not too high. This is consistent with the experimental evidence, which shows that {110} orientations can be quite easily obtained for $SrTiO_3$.

C. Comparison with experimental results

Using the first-principles stability diagrams displayed above, we can now discuss and propose a tentative explanation for the experimental measurements. As anticipated in the Introduction, the $SrTiO_3(110)$ surface was produced and characterized by several groups, showing a great sensitivity to the preparation conditions. In particular, if the $SrTiO_3(110)$ is slightly annealed in ultrahigh vacuum (UHV), at 800 °C (Ref. 15) or at 960 °C for 2 h,[13] the surface exhibits a (1×1) LEED pattern. In contrast, a $(n\times m)$ periodicity is observed when the $SrTiO_3(110)$ surface is annealed at temperatures $T\gtrsim1000$ °C. Therefore, one may guess that (1×1) $SrTiO_3$ (110) surfaces represent local minima of the possibly complex free-energy landscape in a quite wide temperature range. Preliminary calculations on larger cell reconstructions[53] show that some (1×1) phases may remain stable with respect to other reconstructed surfaces. In the following, we mainly discuss the experiments performed on these (1×1) phases.

As far as the composition of the surface is concerned, the authors of Ref. 13 get evidence through Auger measurements of an increasing surface concentration of Sr at the high-temperature annealed surface. Therefore, they conclude for a

lack of strontium for the mildly annealed (1×1) surface, and propose a {100} microfaceted (110)-TiO_2 termination as the corresponding atomic-scale structural model. On the other hand, the STM study of Ref. 15 shows on the (1×1) terminations the presence of rather flat regions where tunneling spectra have metallic character. These findings are consistent with typical Ti^{3+} and Ti^{2+} features in the XPS spectra, as well as a metallic surface state with a Ti $3d$ character as seen in UPS. On the basis of all these observations, and at odds with Ref. 13, they propose a SrTiO termination for the unreconstructed $SrTiO_3$(110) surface, which can account for its flatness and metallic character dominated by Ti-like occupied states.

Relying on our calculations, we argue that these two apparently contradictory models are not necessarily incompatible. On one hand, the UHV Auger measurements may have been carried out in Sr-poor environments, whereas the UHV experimental conditions that have been used in Ref. 15 imply a O-poor environment. Keeping in mind the great sensitivity of the $SrTiO_3$(110) surface to the actual thermodynamic conditions, it is not surprising that its atomic-scale structure may show large variations. According to our calculations (see Fig. 11), the (110)-TiO termination, which can be interpreted as a {100}-TiO_2 microfaceted surface in agreement with the model proposed by Brunen and Zegenhagen,[13] can be obtained in a wide domain corresponding to slightly Sr-poor and O-poor environments. If we assume that the temperature annealing is done in the O-poor condition and, at the same time, rather than Sr-rich conditions (whether one starts from the very beginning with a stoichiometric SrTiO termination without desorbing Sr atoms or the latter ones migrate from the bulk to surface domains of TiO composition remains an open question), a local (110)-SrTiO termination may be obtained as proposed by Bando and co-workers.[15] Indeed, the metallic character of the (110)-SrTiO termination that is due to a surface state mainly of Ti character agrees with the measured UPS spectra. Moreover, as we have previously pointed out for this termination, the anomalous filling of a Ti surface state that is needed for polarity compensation should be associated to special Ti^{n+} features in XPS, with $n<4$.

VI. CONCLUSION

The $SrTiO_3$(110) (1×1) surface was studied in the framework of *ab initio* calculations for the first time, to the best of our knowledge. The number of surface terminations in this ternary compound is larger than in binary compounds, which permits a remarkable variety for mechanisms of polarity compensation. An anomalous filling of the surfaces states takes place at the SrTiO termination with an open-shell electronic structure and at the O_2 termination with in-gap states. If nonstoichiometric O, TiO, and Sr terminations are considered, we obtain for each of them an insulating bulklike electronic structure.

By calculating the surface grand potentials, we obtain four distinct (1×1) stable (110) terminations as functions of the Sr and O chemical potentials. A quite large domain is found for the three nonstoichiometric terminations, especially for the TiO one. This competition between different terminations is also confirmed by the presence of a small domain of stability for the SrTiO termination in simultaneously Sr-rich and O-poor environments.

In conclusion, due to the scarcity of experimental investigations and the observed complexity of the physical and chemical behaviors of the $SrTiO_3$(110) surface, the detailed determination of its atomic and electronic structures still remains an open question. However, our first-principles calculations suggest that even for the unreconstructed (1×1) surfaces, many distinct terminations are likely to appear, according to the precise experimental conditions. In particular, the great dispersion of the experimental results should be connected with such a sensitivity. In the light of our simulations, the available structural models that have been proposed to interpret the measurements seem to be reasonable within a restricted thermodynamic domain. We point out that coupling spectroscopic measurements and structure-sensitive techniques such as near-field microscopies and grazing x-ray diffraction, in very carefully controlled chemical environments may be crucial to get a comprehensive insight into $SrTiO_3$ polar surfaces.

ACKNOWLEDGMENTS

We thank P. Casek for helping us in performing Bader's topological charge analysis. We also ackowledge the financial support from the GDR CNRS ''Interface et Surface Sensible à la Structure'' and from the Laboratoire de Physique des Solides in Orsay, France. The calculations were done on the IBM RS/6000 SP Power3 computer at IDRIS, under project No. 24089.

APPENDIX: BOUNDARY LIMITS FOR THE CHEMICAL POTENTIALS

In this appendix, we derive the range of accessible values for μ_{Sr} and μ_O in the stability diagram of the $SrTiO_3$(110) orientation. The oxygen, titanium, and strontium atoms are assumed to form no condensate on the surface. Consequently, the chemical potential of each species must be lower

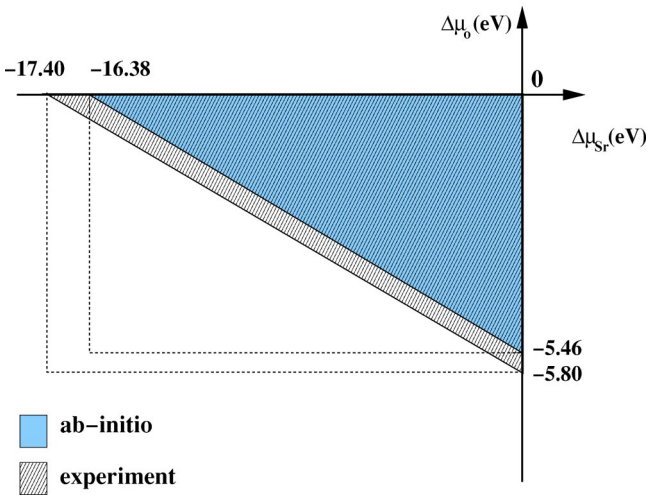

FIG. 13. (Color online) Stability of the strontium titanate phase in a $(\Delta\mu_{Sr};\ \Delta\mu_O)$ plane.

than the energy of an atom in the stable phase of the considered species:

$$\Delta\mu_O = \mu_O - \frac{E^{mol}_{O_2}}{2} < 0, \tag{A1}$$

$$\Delta\mu_{Sr} = \mu_{Sr} - E^{bulk}_{Sr} < 0, \tag{A2}$$

$$\Delta\mu_{Ti} = \mu_{Ti} - E^{bulk}_{Ti} < 0. \tag{A3}$$

We have introduced in these inequations the relative values $\Delta\mu_O$, $\Delta\mu_{Sr}$, and $\Delta\mu_{Ti}$ of the different chemical potentials with respect to E^{bulk}_{Sr}, E^{bulk}_{Ti}, and $E^{mol}_{O_2}/2$, which are the energies of a Ti atom in the hcp bulk metal, of the Sr atom in the bulk cubic structure and of the O atom in the O_2 molecule in the gas phase, respectively. The two first inequations (A1) and (A2) define the upper boundaries of the oxygen and strontium chemical potentials. By combining Eqs. (A3) and (5) in the main text, we obtain the following lower boundaries:

$$\Delta\mu_{Sr} + 3\Delta\mu_O > -E^f_{SrTiO_3}$$

with

$$-E^f_{SrTiO_3} = E^{bulk}_{SrTiO_3} - E^{bulk}_{Ti} - E^{bulk}_{Sr} - \frac{3}{2}E^{mol}_{O_2}. \tag{A4}$$

$E^f_{SrTiO_3}$ is the formation energy of $SrTiO_3$ with respect to the Ti and Sr atoms in their bulk phases, and the O atom in the gas phase, which is positive defined. In order to compute easily this quantity and compare it with the experimental values, we rewrite $E^f_{SrTiO_3}$ in the following way:

$$E^f_{SrTiO_3} = E_{coh} - E^f_{Sr} - E^f_{Ti} - \frac{3}{2}E^f_{O_2} \tag{A5}$$

with all these quantities defined in Sec. II. Our computed value $E^f_{SrTiO_3} = 16.38$ eV is to be compared with the value $E^f_{SrTiO_3} = 17.40$ eV that can be deduced from experimental data. In conclusion, we show the stability of the strontium titanate diagram in a $(\Delta\mu_{Sr}; \Delta\mu_O)$ plane in Fig. 13. As one can see, the *ab initio* calculations only slightly underestimate the size of the stability region.

[1] C. Noguera, *Physics and Chemistry at Oxide Surface* (Cambridge University Press, Cambridge, 1996).
[2] M. Itoh, R. Wang, Y. Inaguma, T. Yamaguchi, Y.-J. Shan, and T. Nakamura, Phys. Rev. Lett. **82**, 5340 (1999).
[3] V. Ravikumar, D. Wolf, and V. Dravid, Phys. Rev. Lett. **74**, 960 (1995).
[4] N.A. Pertsev, A.K. Tagantsev, and N. Setter, Phys. Rev. B **61**, R825 (2000).
[5] W. Zhong and D. Vanderbilt, Phys. Rev. B **53**, 5047 (1996).
[6] C. Cheng, K. Kunc, and M. Lee, Phys. Rev. B **62**, 10 409 (2000).
[7] J. Padilla and D. Vanderbilt, Surf. Sci. **418**, 64 (1998).
[8] E. Heifets, R. Eglitis, E. Kotomin, J. Maier, and G. Borstel, Phys. Rev. B **64**, 235417 (2001).
[9] Q.D. Jiang and J. Zegenhagen, Surf. Sci. **425**, 343 (1999).
[10] T. Kubo and H. Nozoye, Phys. Rev. Lett. **86**, 1801 (2001).
[11] M.R. Castell, Surf. Sci. **505**, 1 (2002).
[12] K. Szot and W. Speier, Phys. Rev. B **60**, 5909 (1999).
[13] J. Brunen and J. Zegenhagen, Surf. Sci. **389**, 349 (1997).
[14] Y. Aiura, H. Bando, Y. Nishira, Y. Haruyama, S. Kodaira, T. Komeda, Y. Sakisaka, T. Maryuama, and H. Kato, *Advances in Superconductivity VI* (Springer, Tokyo, 1994), p. 983.
[15] H. Bando, Y. Aiura, Y. Haruyama, T. Shimizu, and Y. Nishira, J. Vac. Sci. Technol. B **13**, 1150 (1995).
[16] Y. Haruyama, S. Kodaira, Y. Aiura, H. Bando, Y. Nishira, T. Maruyama, Y. Sakisaka, and H. Kato, Phys. Rev. B **53**, 8032 (1996).
[17] H. Bando, Y. Ochiai, Y. Aiura, Y. Haruyama, T. Yasue, and Y. Nishira, J. Vac. Sci. Technol. A **19**, 1938 (2001).
[18] E. Heifets, E. Kotomin, and J. Maier, Surf. Sci. **462**, 19 (2000).
[19] A. Pojani, F. Finocchi, and C. Noguera, Surf. Sci. **442**, 179 (1999).
[20] A. Stashans and S. Serrano, Surf. Sci. **497**, 285 (2002).
[21] A. Wander, F. Schedin, P. Steadman, A. Norris, R. McGrath, T.S. Turner, G. Thornton, and N.M. Harrison, Phys. Rev. Lett. **86**, 3811 (2001).
[22] J.M. Carlsson, Surf. Sci. **22**, 24 (2001).
[23] F. Bottin, F. Finocchi, and C. Noguera, Surf. Sci. (to be published).
[24] P. Hohenberg and W. Kohn, Phys. Rev. **136**, B864 (1964).
[25] J. Perdew and Y. Wang, Phys. Rev. B **45**, 13 244 (1992).
[26] X. Gonze *et al.*, Comput. Mater. Sci. **25**, 478 (2002), see URL http://www.abinit.org
[27] N. Troullier and J. Martins, Phys. Rev. B **43**, 1993 (1991).
[28] L. Kleinman and D.M. Bylander, Phys. Rev. Lett. **48**, 1425 (1982).
[29] M. Fuchs and M. Scheffler, Comput. Phys. Commun. **119**, 67 (1999).
[30] M. Cardona, Phys. Rev. **140**, A651 (1965).
[31] R.W. Godby, M. Schlüter, and L.J. Sham, Phys. Rev. B **37**, 10 159 (1988).
[32] K.H. Weyrich and R. Siems, Z. Phys. B: Condens. Matter **61**, 63 (1985).
[33] G.J. Fischer, Z. Wang, and S.-I. Karato, Phys. Chem. Miner. **20**, 97 (1993).
[34] R.O. Jones and O. Gunnarsson, Rev. Mod. Phys. **61**, 689 (1989).
[35] H.J. Monkhorst and J.D. Park, Phys. Rev. B **13**, 5188 (1976).
[36] N. Mermin, Phys. Rev. **137**, A1441 (1965).
[37] J. Neugebauer and M. Scheffler, Phys. Rev. B **46**, 16 067 (1992).
[38] L. Bengtsson, Phys. Rev. B **59**, 12 301 (1999).
[39] J.C. Boettger, Phys. Rev. B **49**, 16 798 (1994).
[40] V. Fiorentini and M. Methfessel, J. Phys.: Condens. Matter **8**, 6525 (1996).
[41] N. Sai and D. Vanderbilt, Phys. Rev. B **62**, 13 942 (2000).
[42] R. Bader, Chem. Rev. (Washington, D.C.) **91**, 893 (1991).

[43] C. Noguera, A. Pojani, P. Casek, and F. Finocchi, Surf. Sci. **507-510**, 245 (2002).
[44] C. Noguera, J. Phys.: Condens. Matter **12**, R367 (2000).
[45] T. Albaret, F. Finocchi, C. Noguera, and A.D. Vita, Phys. Rev. B **65**, 035402 (2002).
[46] M. C. Desjonquères and D. Spanjaard, *Concept in Surface Physics* (Springer-Verlag, Berlin, 1993), pp. 117–119.
[47] G. Allan and M. Lannoo, Phys. Rev. B **37**, 2678 (1988).
[48] A. Cotton and F. Wilkinson, *Advanced Inorganic Chemistry*, 5th ed. (Wiley, New York, 1980), p. 449, Table 12-1.
[49] X. Wang, A. Chaka, and M. Scheffler, Phys. Rev. Lett. **84**, 3650 (2000).
[50] X. Wang, W. Weiss, S. Shaikhutdinov, M. Ritter, M. Petersen, F. Wagner, R. Schlögl, and M. Scheffler, Phys. Rev. Lett. **81**, 1038 (1998).
[51] O. Dulub, U. Diebold, and G. Kresse, Phys. Rev. Lett. **90**, 016102 (2003).
[52] F. Finocchi (unpublished).
[53] F. Bottin, F. Finocchi, and C. Noguera (unpublished).
[54] The uncertainty associated to this value, because of the number of bulk layers considered and the convergence with respect to the number of k points, is smaller than the thickness convergence one.
[55] The $-TS$ term is neglected for typical temperatures T (S is the entropy of the system).